AMERICAN COLLEGE
of RHEUMATOLOGY
Empowering Rheumatology Professionals

Activated M2 Macrophages Contribute to the Pathogenesis of IgG4-Related Disease via Toll-like Receptor 7/Interleukin-33 Signaling

Noriko Ishiguro,[1] Masafumi Moriyama,[1] [ID] Katsuhiro Furusho,[2] Sachiko Furukawa,[1] Takuma Shibata,[3] Yusuke Murakami,[3] Akira Chinju,[1] A. S. M. Rafiul Haque,[1] Yuka Gion,[4] Miho Ohta,[1] Takashi Maehara,[1] Akihiko Tanaka,[1] Masaki Yamauchi,[1] Mizuki Sakamoto,[1] Keita Mochizuki,[1] Yuko Ono,[1] Jun-Nosuke Hayashida,[1] Yasuharu Sato,[4] Tamotsu Kiyoshima,[1] Hidetaka Yamamoto,[5] Kensuke Miyake,[3] and Seiji Nakamura[1]

Objective. IgG4-related disease (IgG4-RD) is a unique inflammatory disorder in which Th2 cytokines promote IgG4 production. In addition, recent studies have implicated the Toll-like receptor (TLR) pathway. This study was undertaken to examine the expression of TLRs in salivary glands (SGs) from patients with IgG4-RD.

Methods. SGs from 15 patients with IgG4-RD, 15 patients with Sjögren's syndrome (SS), 10 patients with chronic sialadenitis, and 10 healthy controls were examined histologically. TLR family gene expression (TLR-1 through TLR-10) was analyzed by DNA microarray in the submandibular glands (SMGs). Up-regulation of TLRs was confirmed in SGs from patients with IgG4-RD. Finally, the phenotype of human TLR-7 (huTLR-7)–transgenic C57BL/6 mice was assessed before and after stimulation with TLR agonist.

Results. In patients with IgG4-RD, TLR-4, TLR-7, TLR-8, and TLR-9 were overexpressed. Polymerase chain reaction validated the up-regulation of TLR-7 in IgG4-RD compared with the other groups. Immunohistochemical analysis confirmed strong infiltration of TLR-7–positive cells in the SGs of patients with IgG4-RD. Double immunohistochemical staining showed that TLR-7 expression colocalized with CD163+ M2 macrophages. After in vitro stimulation with a TLR-7 agonist, CD163+ M2 macrophages produced higher levels of interleukin-33 (IL-33), which is a Th2-activating cytokine. In huTLR-7–transgenic mice, the focus and fibrosis scores in SMGs, pancreas, and lungs were significantly higher than those in wild-type mice ($P < 0.05$). Moreover, the concentration of serum IgG, IgG1, and IL-33 in huTLR-7–transgenic mice was distinctly increased upon stimulation with a TLR-7 agonist ($P < 0.05$).

Conclusion. TLR-7–expressing M2 macrophages may promote the activation of Th2 immune responses via IL-33 secretion in IgG4-RD.

INTRODUCTION

IgG4-related disease (IgG4-RD) is a recently described disease characterized by elevated serum IgG4 and marked infiltration of IgG4+ plasma cells with hyperplastic ectopic germinal centers (GCs) into multiple organs, including the pancreas, kidney, bile duct, lung, retroperitoneum, prostate, lacrimal glands, and salivary glands (SGs) (1–3). IgG4-RD patients frequently have a history of bronchial asthma and allergic rhinitis with severe eosinophilia and elevated serum IgE levels (4).

It is well known that allergic immune responses are induced by allergen-specific Th2 cytokines, such as interleukin-4 (IL-4), IL-10, and IL-13, which promote isotype switching to both IgG4 and IgE in B cells (5,6). Several studies have

indicated that Th2 cytokines such as IL-4 and IL-10 contribute to the IgG4 production of IgG4-related dacryoadenitis and sialadenitis (IgG4-DS) (7–9) and IgG4-related sclerosing pancreatitis and cholangitis (10). In addition, other adaptive immune cells, including Treg cells (11), follicular helper T cells (12), CD4+ cytotoxic T lymphocytes (13), and IgG4-producing plasmablasts (14), have recently received increasing attention with regard to the pathogenesis of IgG4-RD.

Innate immunity has also recently been shown to play a role in the initiation of IgG4-RD. We previously described the accumulation of CD163+ M2 macrophages in multiple organs from patients with IgG4-RD, indicating that these cells may contribute to the fibrosis associated with IgG4-RD through the production of profibrotic factors (CCL18 and IL-10) (15) and the activation of Th2 immune responses via IL-33 secretion (16). In addition, several studies have indicated that BAFF secreted by macrophages and basophils induces IgG4 production by B cells via activation of Toll-like receptors (TLRs) (17,18). Although BAFF was discovered originally as a cytokine that potentiates B cell maturation and immunoglobulin production (19), the BAFF-induced immunoglobulin subset was not restricted to IgG4; therefore, the immunopathogenesis of IgG4-RD via the TLR pathway remains unclear.

TLRs are a family of transmembrane receptors that play a crucial role in the activation of innate immunity against invading pathogens (20,21), as well as the development of antigen-specific acquired immunity (22,23). Interestingly, inappropriate signaling by TLRs triggers the polyclonal expansion of B cells that occurs after exposure to infectious agents and then exacerbates autoimmune diseases (24). In this study, we thus sought to characterize the expression of the TLR family in SGs from patients with IgG4-RD and the phenotype of TLR-transgenic mice to clarify the contribution of TLRs to the pathogenesis of IgG4-RD.

PATIENTS AND METHODS

Study participants. The study design and methods were approved by the Institutional Review Board of the Center for Clinical and Translational Research of Kyushu University Hospital (IRB serial nos. 25-287 and 26-86) and followed the tenets of the Declaration of Helsinki. The methods were carried out in accordance with the approved guidelines. All patients or their relatives gave their informed consent within the written treatment contract on admission and therefore prior to their inclusion in the study.

SG samples and peripheral blood mononuclear cells (PBMCs) were obtained from patients referred to the Department of Oral and Maxillofacial Surgery, Kyushu University Hospital between 2010 and 2016. The study included 15 patients with IgG4-RD (11 men and 4 women; mean ± SD age 63.6 ± 10.3 years), 15 patients with primary Sjögren's syndrome (SS) (15 women; age 54.3 ± 17.6 years), 10 patients with chronic sialadenitis (4 men and 6 women; age 49.1 ± 21.6 years), and 10 healthy controls (5 men and 5 women; age 62.1 ± 13.6 years). Clinical and serologic

profiles of the patients with IgG4-RD are available upon request from the corresponding author.

Patients with IgG4-RD and patients with SS underwent open SG biopsies, as described by Moriyama et al (25), while patients with chronic sialadenitis underwent an extraction of SGs. IgG4-RD was diagnosed according to both the "Comprehensive diagnostic criteria for IgG4-related disease" (26) and "Diagnostic criteria for IgG4-DS" (27). All patients with IgG4-RD showed characteristic histopathologic findings, including marked infiltration of IgG4-positive plasma cells, severe fibrosis, and formation of multiple ectopic GCs, and had never been treated with steroids or any other immunosuppressants. SS was diagnosed according to both the 1999 criteria for SS from the Research Committee of the Ministry of Health, Labour and Welfare of the Japanese Government (28) and the American College of Rheumatology/European League Against Rheumatism 2016 Classification Criteria for primary SS (29). All patients with SS had lymphocytic infiltration in the SGs, had no other autoimmune diseases, and had never been treated with steroids or any other immunosuppressants. There was no documented history of HIV, human T lymphotropic virus type 1, hepatitis B virus, or hepatitis C virus infection in any of the patients. None of the patients had evidence of malignant lymphoma at the time of the study. For comparison, tonsils and lymph nodes were obtained from patients with oral squamous cell carcinoma at tumor resection. These samples from patients with oral squamous cell carcinoma were histologically normal and lacked clinical evidence of metastasis and radiation therapy.

Extraction of RNA and synthesis of complementary DNA (cDNA). Total RNA was prepared from SGs by the acidified guanidinium–phenol–chloroform method as previously described (30). One microgram of total RNA was prepared and used for the synthesis of cDNA, and then RNA was incubated for 1 hour at 42°C with 20 units of RNase inhibitor (Promega), 0.5 μg of oligo-1218 (Pharmacia), 0.5 mM deoxyribonucleotide triphosphate (Pharmacia), 10 mM of dithiothreitol, and 100 units of RNA reverse transcriptase (Life Technologies).

Gene expression microarrays. According to the manufacturers' instructions, complementary RNA was amplified and labeled using a Low Input Quick Amp Labeling Kit (Agilent), and hybridized to SurePrint G3 Human Gene Expression Microarrays 8 60K v2 (Agilent) (DNA chip including 60,000 genes). All hybridized microarray slides were scanned using an Agilent scanner. Relative hybridization intensities and background hybridization values were calculated using Agilent Feature Extraction Software (version 9.5.1.1) as previously described (31).

Quantitative estimation of messenger RNA (mRNA) by real-time polymerase chain reaction (PCR). The resulting cDNA was amplified using LightCycler FastStart DNA Master mix SYBR Green III (Roche Diagnostics) in a LightCycler real-time

PCR instrument (version 3.5; Roche Diagnostics). The levels of mRNA for TLR-7, TLR-8, TLR-9, and IL-33 were analyzed. Target mRNA levels were expressed relative to β-actin as the housekeeping gene. Primer sequences used are available upon request from the corresponding author. All analyses were performed in triplicate.

Immunohistochemical analysis. Serial 4-μm sections were cut from formalin-fixed and paraffin-embedded SG tissue and stained with a conventional avidin–biotin complex technique as previously described (30). Antibodies used included anti-CD68 (catalog no. ab955; Abcam), anti-CD163 (catalog no. NCL-CD163; Leica Biosystems), anti-CD123 (catalog no. NCL-L-CD123; Leica Biosystems), anti–TLR-8 (catalog no. 85859; Abcam), anti–TLR-9 (catalog no. 134368; Abcam), and anti-IL-33 (catalog no. 54385; Abcam) mouse monoclonal antibodies; anti-CD11c (catalog no. 52632; Abcam), and anti–TLR-7 (catalog no. 124928; Abcam) rabbit monoclonal antibodies; anti-CD317 (catalog no. DDX0390p-100; Novus) rat monoclonal antibodies; and anti–TLR-10 (catalog no. 53631; Abcam), anti-CD206 (catalog no. AF2534; R&D Systems), and anti-IgG1 (catalog no. 97236; Abcam) goat polyclonal antibodies. Tissue sections were sequentially incubated with primary antibodies for 2.5 hours and then with biotinylated anti-mouse, anti-rabbit, anti-rat, or anti-goat IgG secondary antibodies (Vector), followed by avidin–biotin–horseradish peroxidase complex (Vector), and 3,3′-diaminobenzidine (Vector). Mayer's hematoxylin was used for counterstaining.

For double immunofluorescence analysis, formalin-fixed and paraffin-embedded sections of submandibular glands (SMGs) were stained using an Opal 4-Color Manual IHC Kit (catalog #NEL810001KT; PerkinElmer). The following primary antibodies were used: anti-CD163, anti-CD123, and anti–TLR-7. Photomicrographs were obtained using a light microscope equipped with a digital camera (BZ-9000 series; Keyence).

Cell culture and stimulation of human CD163+ M2 macrophages in vitro. PBMCs were obtained from a healthy donor, and CD14+ monocytes were isolated using an EasySep Human Monocyte Isolation Kit (StemCell Technologies). Cells (5×10^6 cells/ml) were cultured using a CellXVivo Human M2 Macrophage Differentiation Kit (R&D Systems) for 6 days in a humidified chamber with 5% CO_2 at 37°C. Differentiated M2 macrophages were dissociated and collected.

Next, collected cells were then counted and separated in three 15-ml tubes, followed by incubation with fluorescein isothiocyanate (FITC)–conjugated anti-human CD163 antibodies (BioLegend) for 10 minutes in the dark at 4°C. Samples were washed in MACS buffer (Miltenyi Biotec) and incubated with Anti-FITC MicroBeads (Miltenyi Biotec) for 15 minutes at 4°C. Samples were washed, and CD163+ cells were separated by manual magnetic-activated cell sorting procedure with a MiniMACS Starting Kit (Miltenyi Biotec), and were stimulated with R848. The supernatants were subjected to analysis.

Human TLR-7–transgenic/mouse TLR-7–deficient (huTLR-7–transgenic/mTLR-7$^{-/-}$) mice and in vivo treatment. The in vivo function of huTLR-7 was examined using TLR-7$^{-/-}$ mice and huTLR-7–transgenic/mTLR-7$^{-/-}$ mice on a C57BL/6 background. First, we generated Gt(ROSA)26Sor$^{huTLR7/+}$ mice (details are available upon request from the corresponding author). Briefly, CAG-STOP-eGFP-ROSA26TV Targeting vector (a kind gift from Yoshiteru Sasaki) with huTLR-7 coding sequence was electroporated into C57BL/6N mouse–derived JM8.A3N1 embryonic stem cells (ESCs). Neomycin-resistant ESC clones were screened by Southern blot analysis using a 5′ external probe and PCR using a 5′ external primer (5′-TCCTCA GAGAGCCTCGGCTAGGTAG-3′) and neomycin primer (5′- AA TGGCCGCTTTTCTGGATTCATC-3′), and then a homologous recombinant ESC clone was injected into C57/BL6N mouse–derived blastocysts to produce chimeric mice. Since the targeted allele enables CAG promoter–driven expression of human TLR-7 and green fluorescent protein (GFP) after removal of the floxed neomycin cassette by recombinases, male chimeric mice were crossed with female CAG-Cre–transgenic mice. Finally, Gt(ROSA)26Sor$^{huTLR-7/+}$ mice were crossed with mTLR-7$^{-/-}$ mice, and mTLR-7$^{-/-}$/Gt(ROSA)26Sor$^{huTLR-7/+}$ (huTLR-7–transgenic) mice were subjected to in vivo experiments. For TLR-7 ligand treatment of mice, the skin on the ears was topically treated, 3 times weekly, with 100 μg of resiquimod (R848; ChemScene Chemicals) in 100 μl of acetone.

Histologic analysis in huTLR-7–transgenic/mTLR-7$^{-/-}$ mice. Four-micron sections of mouse SMG, pancreas, kidney, lung, and liver were prepared and stained with hematoxylin and eosin (H&E) for conventional histologic examination. The degree of lymphocytic infiltration in the specimens was judged by focus scoring. The standardized score used is the number of focal inflammatory cell aggregates containing 50 or more mononuclear cells in each 4 μm^2 area of SG tissue (32,33).

Evaluation of the severity of fibrosis in huTLR-7–transgenic/mTLR-7$^{-/-}$ mice. To evaluate fibrosis histologically, Masson's trichrome staining (Polysciences) was performed. Briefly, 4-μm formalin-fixed, paraffin-embedded sections were prepared and stained. Connective and fibrotic tissues were selectively stained blue, whereas nuclei were stained dark brown to black by Weigert's iron hematoxylin and the cytoplasm was stained red. The fibrosis scores in mouse SMGs, pancreas, kidney, lung, and liver were defined as the ratio of the fibrotic area (blue) to the whole stained area in a 4 μm^2 field of view, from 5 different areas.

Induction of bone marrow–derived macrophages. Bone marrow cells from mTLR-7$^{-/-}$ and huTLR-7–transgenic mice on a C57BL/6 background were cultured with 100 ng/ml macrophage colony-stimulating factor (catalog no. 315-02; PeproTech) for 7 days.

Flow cytometric analysis. Prepared cells were subjected to flow cytometric analysis using an LSRFortessa X-20 system (Becton Dickinson). Bone marrow–derived macrophages were stained with anti-CD11b monoclonal antibody (clone M1/70). To detect GFP in bone marrow–derived macrophages (CD11b+), a blue laser was used. Flow cytometry data were analyzed using FlowJo software.
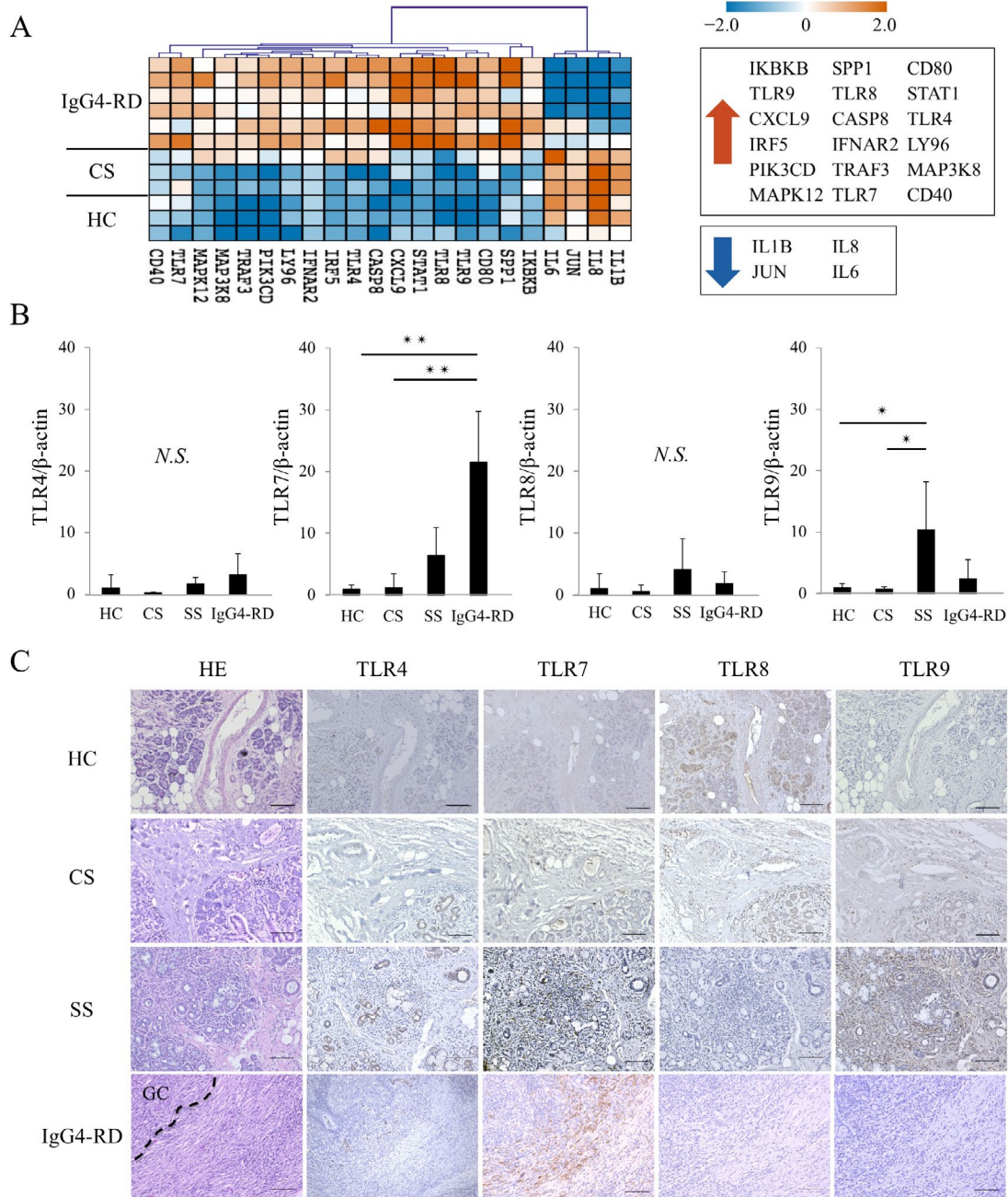
Figure 1. Toll-like receptor (TLR)–related gene expression patterns in salivary glands (SGs) from patients with IgG4-related disease (IgG4-RD). **A**, Heatmap depicting differentially expressed TLR-related genes in submandibular glands (SMGs) from patients with IgG4-RD (n = 6), patients with chronic sialadenitis (CS; n = 3), and healthy controls (HCs; n = 3). Only genes up-regulated or down-regulated by at least 2-fold are shown. **B**, Quantitative polymerase chain reaction analysis of TLR-4, TLR-7, TLR-8, and TLR-9 in SGs from healthy controls (n = 10), patients with chronic sialadenitis (n = 10), patients with Sjögren's syndrome (SS; n = 15), and patients with IgG4-RD (n = 15). Bars show the mean ± SD. * = $P < 0.05$; ** = $P < 0.01$ by Kruskal-Wallis test. NS = not significant. **C**, Distribution of candidate TLRs in SMGs from representative healthy controls and patients with chronic sialadenitis, patients with SS, and patients with IgG4-RD. Sections were stained with hematoxylin and eosin (H&E) and for TLR-4, TLR-7, TLR-8, and TLR-9. Outlined area indicates a germinal center (GC). Mayer's hematoxylin (blue) counterstained; bars = 100 μm.

Stimulation of bone marrow–derived macrophages. Bone marrow–derived macrophages (5×10^4 cells/well) were seeded in 96-well plates and stimulated with R848 (catalog no. tlrl-r848; InvivoGen) for 24 hours. The culture supernatant was collected and subjected to enzyme-linked immunosorbent assay (ELISA) to detect cytokines.

ELISA. Serum levels of total IgG, IgG1, and IgG2a in mice were analyzed using a total IgG mouse uncoated ELISA kit with plates (catalog no. 88-50400-88; eBioscience), an IgG1 mouse uncoated ELISA kit with plates (catalog no. 88-50410-88; eBioscience), and an IgG2a mouse coated ELISA kit with plates (catalog no. ab133046; Abcam), respectively. IL-6, IL-12p40, and IL-33 in mice were detected by mouse IL-6 ELISA Ready-SET-Go! (catalog no. 88-7064-88; ThermoFisher Scientific), mouse IL-12p40 ELISA Ready-SET-Go! (catalog no. 88-7120-77; ThermoFisher Scientific), and IL-33 mouse uncoated ELISA kit plates (catalog no. GWB-SKR038; GenWay Biotech), respectively. IL-33 in humans was detected using a human IL-33 ELISA Kit (catalog no. ab223865; Abcam).

Statistical analysis. The significance of differences between groups was determined using chi-square test, Student's *t*-test, Mann-Whitney U test, and Kruskal-Wallis tests, and Spearman's rank correlation test was used to test correlations between groups. *P* values less than 0.05 were considered significant. All statistical analyses were performed using JMP software (V.8; SAS Institute).

RESULTS

Gene expression profiles of the TLR family in the SMGs. DNA microarray analysis was performed to compare gene expression profiles of SMG samples from healthy controls and patients with IgG4-RD or chronic sialadenitis. A heatmap was used to elucidate and visualize the differences in gene expression levels among patients with IgG4-RD, those with chronic sialadenitis, and controls (details are available upon request from the corresponding author). The differences in TLR-related gene expression between patients with IgG4-RD and those with chronic sialadenitis are shown in Figure 1A. The genes associated with TLR-4, TLR-7,
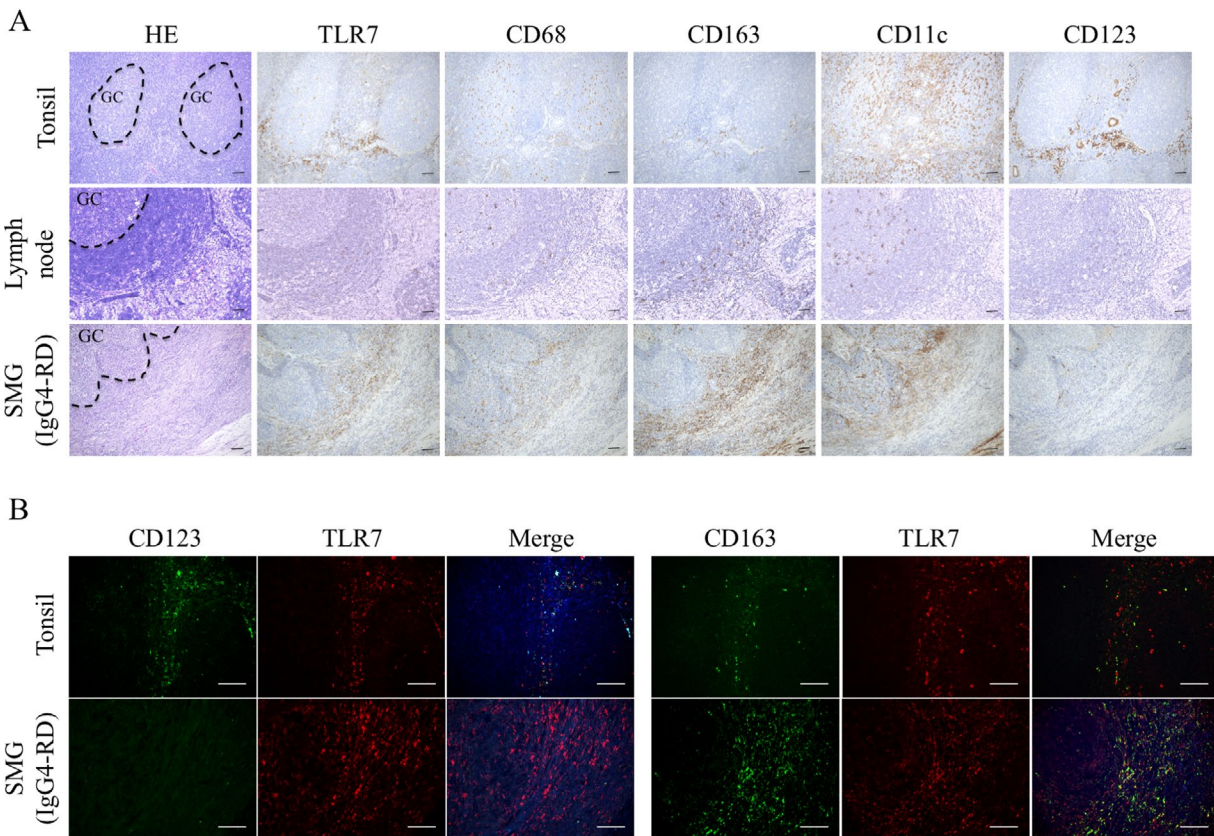
Figure 2. Identification of TLR-7–expressing cells in SMGs from patients with IgG4-RD and in normal secondary lymphoid organs from patients with oral squamous cell carcinoma. **A**, Staining of serial sections of normal tonsil, normal lymph node, and IgG4-RD SMGs with H&E, and for TLR-7, CD68 as a marker of both M1 and M2 macrophages, CD163 as a marker of M2 macrophages, CD11c as a marker of myeloid dendritic cells, and CD123 as a marker of plasmacytoid dendritic cells. Outlined areas indicate GCs. Mayer's hematoxylin (blue) counterstained; bars = 100 μm. **B**, Double immunostaining for TLR-7 (red), CD123 (green), and CD163 (green) in normal tonsil and SMGs from representative patients with IgG4-RD. DAPI (blue) counterstained; bars = 50 μm. See Figure 1 for definitions.

TLR-8, and TLR-9 were expressed to a higher extent in samples from IgG4-RD patients than those from patients with chronic sialadenitis or healthy controls. The expression of these candidate TLR genes was subsequently validated using quantitative real-time PCR by increasing the number of cases. As shown in Figure 1B, we found that the expression levels of mRNA for TLR-7 were significantly higher in SGs from patients with IgG4-RD compared with those from healthy controls or patients with chronic sialadenitis or SS.

Expression of candidate TLRs in the SGs. To evaluate the distribution of candidate TLRs, including TLR-4, TLR-7, TLR-8, and TLR-9, in SG specimens from patients with IgG4-RD, patients with chronic sialadenitis, patients with SS, and healthy controls, histologic analysis was carried out. Representative findings are shown in Figure 1C. Expression of TLR-7 was only detected in infiltrating inflammatory cells, identified morphologically in samples from patients with SS and patients with IgG4-RD but not those from patients with chronic sialadenitis or controls. In addition, patients with IgG4-RD showed strong infiltration of these positive cells around ectopic GCs compared with patients with SS. The other candidate TLRs were rarely seen in any of the samples.

Identification of TLR-7–expressing cells in the SMGs and normal secondary lymphoid organs. Since TLR-7 is expressed on macrophages and dendritic cells (DCs) in secondary lymphoid organs (34), we examined the distribution of macrophages (CD68+, CD163+), DCs (CD11c+, CD123+), and TLR-7 in the SMGs from patients with IgG4-RD and in normal secondary lymphoid organs such as lymph nodes and tonsils. Expression of CD68 and CD163 was strongly detected around ectopic GCs and fibrotic areas in IgG4-RD tissues. In the normal secondary lymphoid organs, expression of CD68 was also strongly detected in and around ductal ectopic GCs, whereas expression of CD163 was rarely detected around ectopic GCs. Expression of CD11c was strongly detected in and around ectopic GCs in both IgG4-RD tissues and normal secondary lymphoid organs. Expression of CD123 was rarely seen in IgG4-RD tissues, but CD123 was detected around ectopic GCs and in ductal epithelial cells in normal secondary lymphoid organs. Finally, expression of TLR-7 was strongly detected around ectopic GCs and fibrotic areas in IgG4-RD tissues, whereas expression of TLR-7 was detected only around ectopic GCs in normal secondary lymphoid organs (Figure 2A).

To clarify which cells expressed TLR-7 in IgG4-RD tissues, double immunofluorescence staining for TLR-7 (red) and CD163 or CD123 (green) was performed. Using this approach, TLR-7–positive cells mainly colocalized with CD123-positive cells in secondary lymphoid organs. In contrast, in IgG4-RD tissues, TLR-7–positive cells mainly colocalized with CD163-positive cells (Figure 2B). This is consistent with macrophages, particularly M2 macrophages, expressing TLR-7 in IgG4-RD tissues.

Relationship between TLR-7 and IL-33 expression in the SGs. As mentioned above, our recent data indicate that M2 macrophages might contribute to aberrant activation of Th2 immune responses and fibrosis via production of IL-33 (15,16). IL-33 is a recently described cytokine and directly stimulates ST2-expressing immune cells, including Th2 cells, mast cells, eosinophils, and basophils, to secrete Th2 cytokines (35). Recently, in a mouse model where influenza infection acutely induces airway hyperreactivity, TLR-7 stimulation promoted IL-33 production by alveolar macrophages in the lung (36). In addition, TLR-7$^{-/-}$ mice developed a limited airway hyperreactivity response to influenza infection (37). Thus, we examined the association between IL-33 and candidate TLRs in IgG4-RD tissues. The expression levels of mRNA for IL-33 in SGs from patients with IgG4-RD were significantly higher than those in SGs from patients with chronic sialadenitis and controls (Figure 3A).

To evaluate the distribution of IL-33, SG specimens from patients with SS, patients with IgG4-RD, patients with chronic sialadenitis, and healthy controls were characterized immunohistochemically. Representative sections are shown in Figure 1C. Expression of IL-33 was detected in all samples in the ductal epithelial cells, while IL-33 was also detected in infiltrating inflammatory cells around ectopic GCs in patients with IgG4-RD (Figure 3B). Next, the relationships between expression levels of mRNA for IL-33 and candidate TLRs in SGs from patients with IgG4-RD were examined, and the expression of mRNA for IL-33 was positively correlated with expression of mRNA for TLR-7 but not with expression of mRNA for TLR-4, TLR-8, or TLR-9 (Figure 3C). Finally, CD163+ M2 macrophages isolated from PBMCs (Figure 3D) were found to enhance production of IL-33 in a dose-dependent manner after stimulation with TLR-7 agonist (Figure 3E). This suggested that activation of TLR-7 might induce the release of IL-33 from M2 macrophages.

Phenotype of affected organs in huTLR-7–transgenic/mTLR-7$^{-/-}$ mice. Since our current data suggest that TLR-7 might play a key role in the initiation of IgG4-RD, we examined the phenotype of Gt(ROSA)26Sor$^{huTLR-7/+}$/mTLR-7$^{-/-}$ mice (Figure 4A). Histologic examination was undertaken of organs relevant for IgG4-RD, including the SMGs, pancreas, kidney, lung, and liver, in huTLR-7–transgenic/mTLR-7$^{-/-}$ and wild-type (WT) mice. There were no significant differences in the weights of each organ between huTLR-7–transgenic/mTLR-7$^{-/-}$ mice and WT mice (Figure 4B). Representative histologic findings in each organ from huTLR-7–transgenic/mTLR-7$^{-/-}$ and WT mice are shown in Figure 4C. The degree of lymphocytic infiltration was evaluated by focus score, and the focus scores in the SMGs,
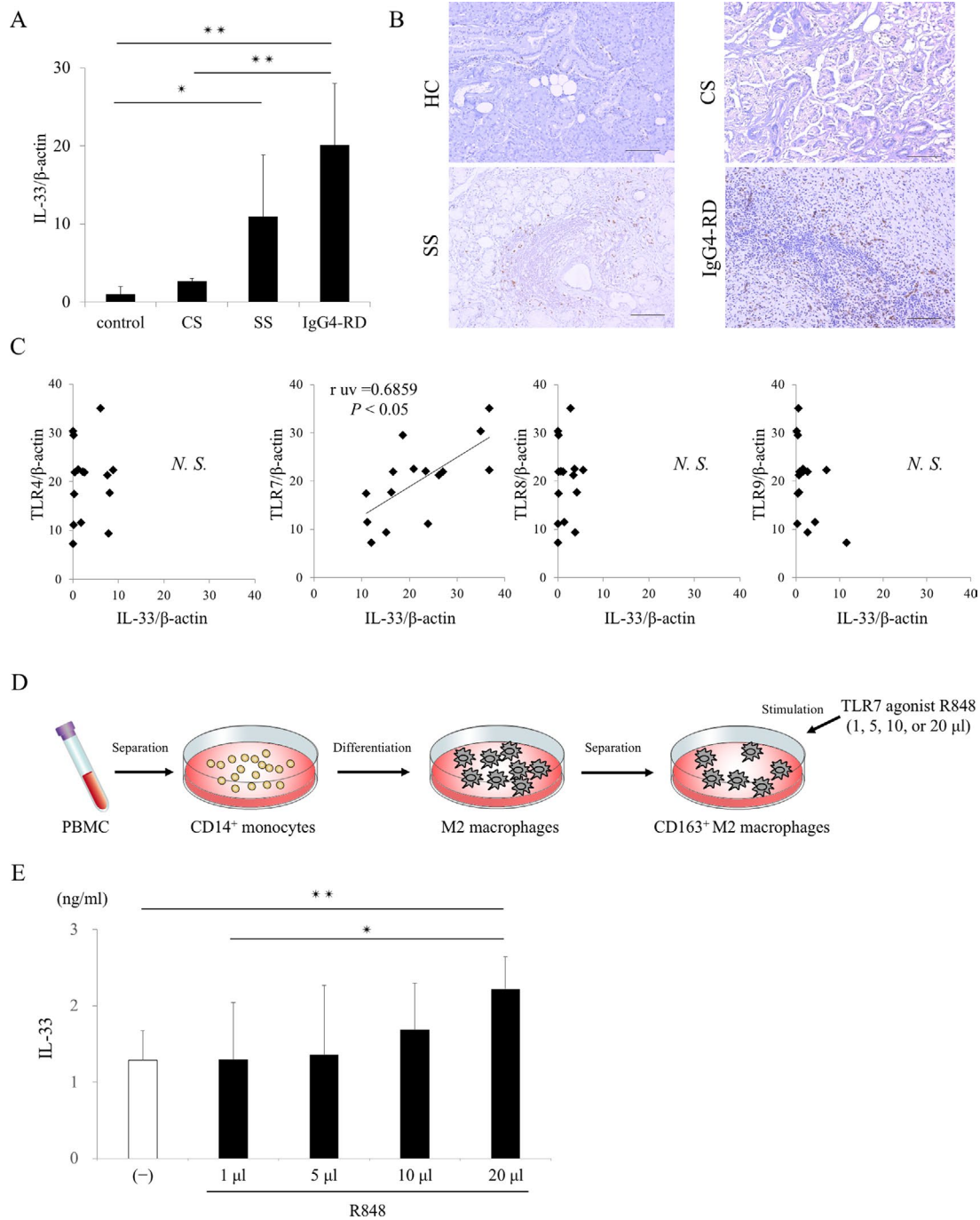
Figure 3. Expression of interleukin-33 (IL-33) and candidate TLRs in SGs from patients with IgG4-RD. **A**, Expression levels of mRNA for IL-33 in SGs from healthy controls (n = 10), patients with chronic sialadenitis (n = 10), patients with SS (n = 15), and patients with IgG4-RD (n = 15). **B**, Distribution of IL-33 in SGs from a representative healthy control, patient with chronic sialadenitis, patient with SS, and patient with IgG4-RD. Mayer's hematoxylin (blue) counterstained; bars = 100 μm. **C**, Correlation between expression levels of IL-33 mRNA and candidate TLRs in SGs from patients with IgG4-RD (n = 15), as determined by Spearman's rank correlation test. **D**, Schematic illustration of the extraction of CD163+ M2 macrophages stimulated with TLR-7 agonist R848. Cells were cultivated as described in Patients and Methods. PBMC = peripheral blood mononuclear cell. **E**, Production of IL-33 by CD163+ M2 macrophages stimulated with R848, as determined by enzyme-linked immunosorbent assay. IL-33 levels increased in a concentration-dependent manner. In **A** and **E**, bars show the mean ± SD. * = $P < 0.05$; ** = $P < 0.01$ by Kruskal-Wallis test. See Figure 1 for other definitions.

pancreas, and lungs from huTLR-7–transgenic/mTLR-7^{−/−} mice were significantly greater than in WT mice (Figure 4D). In addition, to evaluate the degree of fibrosis in each organ, specimens were stained by Masson's trichrome staining. The huTLR-7–transgenic/mTLR-7^{−/−} mice showed severe fibrosis in the lung and cordlike fibrosis in the SMGs and pancreas (Figure 4E).
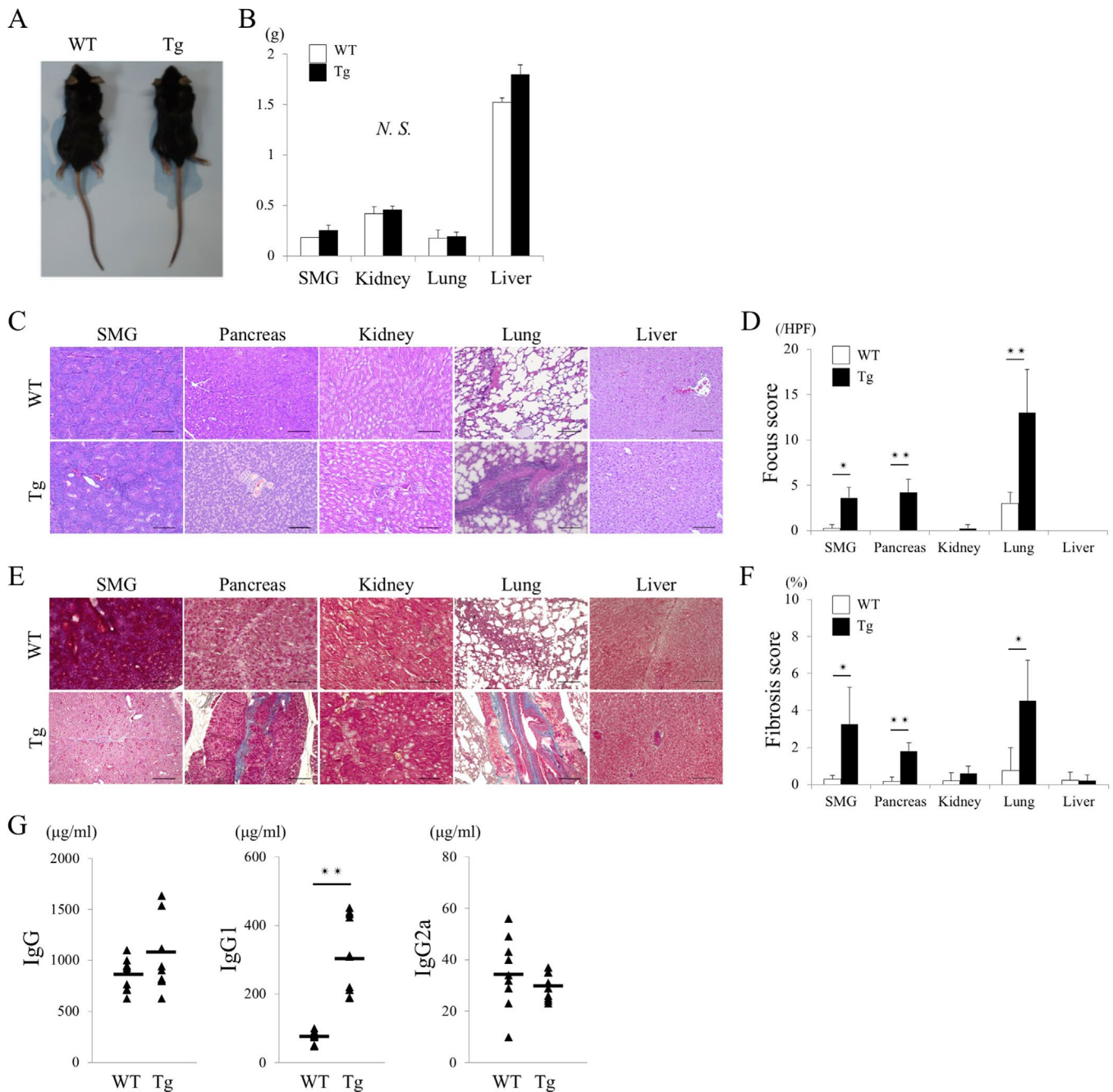
Figure 4. Pathologic and serologic findings in human TLR-7–transgenic/mouse TLR-7–deficient (huTLR-7–transgenic/mTLR-7$^{-/-}$) mice on a C57BL/6 background. **A**, A wild-type (WT) C57BL/6 mouse and an huTLR-7–transgenic/mTLR-7–/– (transgenic [Tg]) mouse at 4 weeks old. **B**, Weight of SMGs, kidneys, lungs, and liver in 4-week-old WT mice (n = 5) and transgenic mice (n = 5). Bars show the mean ± SD. **C**, H&E-stained sections of SMGs, pancreas, kidneys, lungs, and liver from representative WT and transgenic mice. Bars = 100 μm. **D**, Focus score for each organ in WT mice (n = 5) and transgenic mice (n = 5). The focus score was estimated as described in Patients and Methods. Bars show the mean ± SD. HPF = high-power field. **E**, Masson's trichrome–stained sections of SMGs, pancreas, kidneys, lungs, and liver from representative WT and transgenic mice. Masson's trichrome was used to stain nuclei (purple), cytoplasm (red), and collagen (connective or fibrotic tissue; blue) Bars = 100 μm. **F**, Fibrosis score for each organ in WT mice (n = 5) and transgenic mice (n = 5). The fibrosis score was calculated from Masson's trichrome staining as described in Patients and Methods. Bars show the mean ± SD. **G**, Serum IgG, IgG1, and IgG2a levels in WT mice (n = 10) and transgenic mice (n = 10), as determined by enzyme-linked immunosorbent assay. Symbols represent individual mice; horizontal lines show the mean. * = $P < 0.05$; **= $P < 0.01$ by Mann-Whitney U test. See Figure 1 for other definitions.
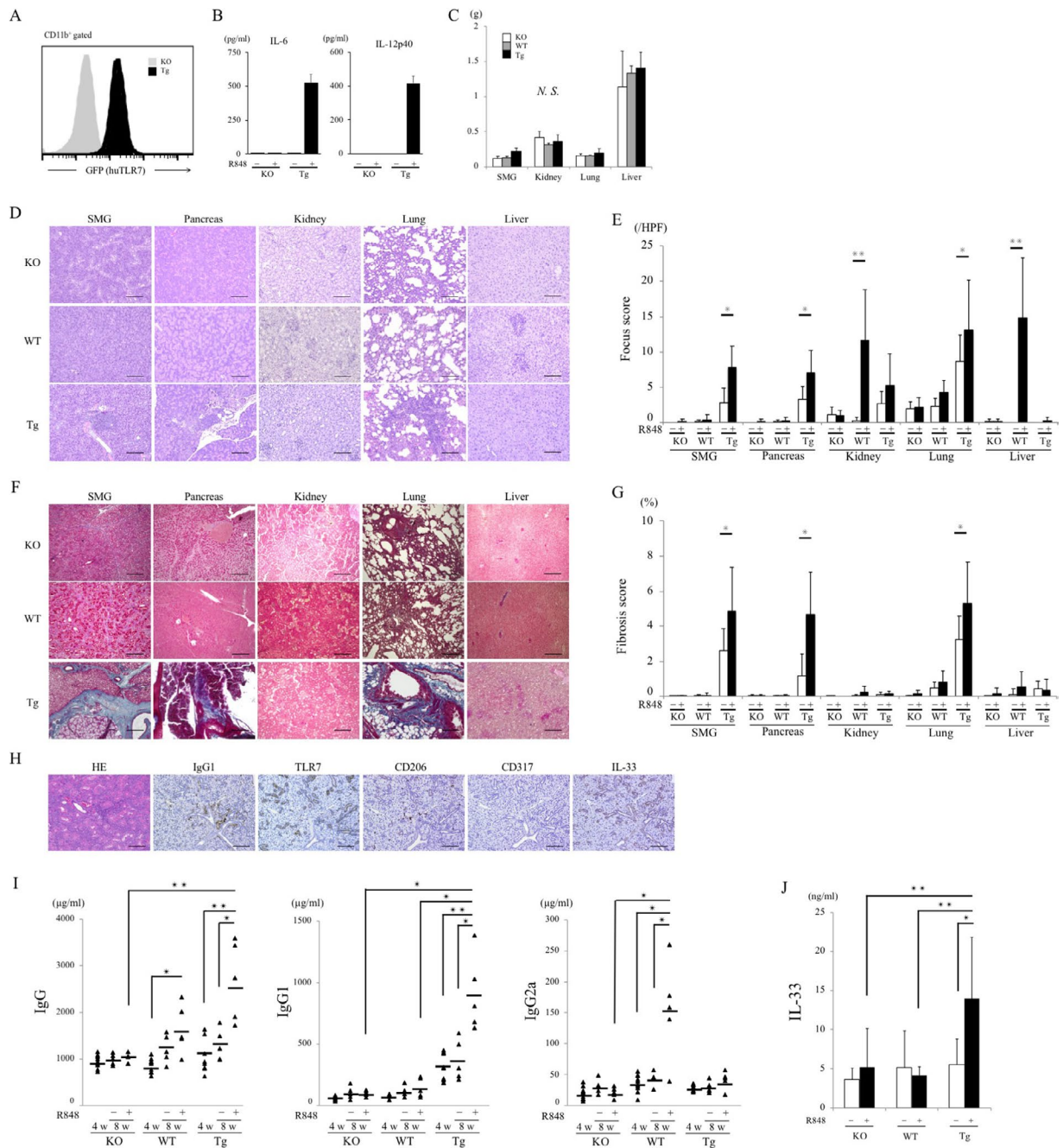
Figure 5. Effects of TLR-7 agonist R848 in transgenic mice. **A**, Detection of GFP in bone marrow–derived macrophages (BMMs) from mTLR-7–/– (knockout [KO]) mice and transgenic (Tg) mice by flow cytometric analysis, after staining with anti-CD11b antibody. At least 2 independent experiments were performed. **B**, Interleukin-6 (IL-6) and IL-12p40 levels in BMMs from knockout mice and transgenic mice left unstimulated or stimulated with R848. After 24 hours of incubation, IL-6 and IL-12p40 were detected in culture medium by enzyme-linked immunosorbent assay (ELISA). Results are from triplicate wells. At least 2 independent experiments were performed. **C**, Weight of SMGs, kidneys, lungs, and liver in 8-week-old knockout, wild-type (WT), and transgenic mice treated with topical R848 for 4 weeks (n = 8 per group). **D** and **F**, H&E-stained (**D**) and Masson's trichrome–stained (**F**) sections of SMGs, pancreas, kidneys, lungs, and liver from representative 8-week-old R848-treated knockout, WT, and transgenic mice. Bars = 100 μm. **E** and **G**, Focus score (**E**) and fibrosis score (**G**) for each organ in 8-week-old knockout, WT, and transgenic mice left untreated or treated with R848 (n = 8 per group). The fibrosis score was calculated from Masson's trichrome staining as described in Patients and Methods. HPF = high-power field. **H**, Serial sections of SMGs from a representative 8-week-old R848-treated transgenic mouse, stained with H&E and for IgG1, TLR-7, CD206, CD317, and IL-33. Mayer's hematoxylin (blue) counterstained; bars = 100 μm. **I**, Serum IgG, IgG1, and IgG2a levels in knockout, WT, and transgenic mice (n = 10 per group) before and after R848 treatment, as determined by ELISA. Symbols represent individual mice; horizontal lines show the mean. **J**, Serum IL-33 levels, determined by ELISA, in knockout, WT, and transgenic mice left untreated or treated with R848 (n = 10 per group). In **B**, **C**, **E**, **G**, and **J**, bars show the mean ± SD. * = P < 0.05; ** = P < 0.01 by Mann-Whitney U test in **E** and **G**; by Kruskal-Wallis test in **C**, **I** and **J**. See Figure 1 for other definitions.

The fibrosis scores for the SMGs, pancreas, and lungs from huTLR-7–transgenic/mTLR-7$^{-/-}$ mice were significantly higher than those in WT mice (Figure 4F).

Serum IgG1 levels in 4-week-old huTLR-7–transgenic/mTLR-7$^{-/-}$ mice were significantly higher than those in 4-week-old WT mice, while there was no significant difference in serum IgG or IgG2a levels between huTLR-7–transgenic/mTLR-7$^{-/-}$ and WT mice (Figure 4G).

Response to a TLR-7 agonist in huTLR-7–transgenic/mTLR-7$^{-/-}$ and WT mice. To test the in vivo responsiveness of huTLR-7–transgenic/mTLR-7$^{-/-}$ mice to an agonist of TLR-7, we applied the TLR-7 agonist R848 to their right ears, 3 times weekly for 4 weeks. Bone marrow–derived macrophages (CD11b+ cells) prepared from Gt(ROSA)26Sor$^{huTLR-7/+}$ TLR-7$^{-/-}$ mice expressed GFP (Figure 5A) and produced IL-6 and IL-12 p40 in response to the TLR-7 ligand R848 (Figure 5B), demonstrating that Gt(ROSA)26Sor$^{huTLR-7/+}$ TLR-7$^{-/-}$ mice enable us to study human TLR-7 responses in vivo. Once again, mouse SMGs, pancreas, kidney, lung, and liver were collected. There were no significant differences in the weights of the organs among 8-week-old R848-treated huTLR-7–transgenic/mTLR-7$^{-/-}$ mice, mTLR-7$^{-/-}$ mice, and WT mice (Figure 5C). Histologic examination of the SMGs, pancreas, and lung from R848-treated huTLR-7–transgenic/mTLR-7$^{-/-}$ mice revealed marked inflammation and fibrosis, while there was marked inflammation and fibrosis in the kidney and liver from R848-treated WT mice (Figures 5D and F). In R848-treated huTLR-7–transgenic/mTLR-7$^{-/-}$ mice, the focus score and fibrosis score for the SMGs, pancreas, and lung were significantly increased after R848 stimulation (Figures 5E and G). In contrast, in R848-treated WT mice, the focus scores for the kidney and liver were significantly increased after R848 stimulation (Figure 5E), but the fibrosis score remained unchanged for all organs (Figure 5G). Immunohistochemical analysis demonstrated focal accumulation of CD206+ cells (marker for M2 macrophages in mice), IgG1+ plasma cells, and IL-33+ cells around ectopic GCs in the SMGs, while there were no CD317+ cells (marker for plasmacytoid DCs in mice) in the SMGs (Figure 5H).

Beginning 4 weeks after topical R848 treatment, serum IgG, IgG1, and IgG2a levels in knockout mice remained unchanged. Interestingly, serum IgG2a levels were significantly elevated only in WT mice, while serum IgG and IgG1 levels were significantly elevated only in huTLR-7–transgenic/mTLR-7$^{-/-}$ mice (Figure 5I). Mouse IgG1 is considered a functional equivalent of human IgG4. Moreover, serum IL-33 levels were significantly elevated only in huTLR-7–transgenic/mTLR-7$^{-/-}$ mice (Figure 5J). Thus, huTLR-7 activation through topical TLR-7 agonist treatment might lead to the manifestation of IgG4-RD.

DISCUSSION

M2 macrophages are typically degenerated by stimulation with the Th2 cytokines IL-4 and IL-13 (38). Notably, in allergic

regions, infiltrating inflammatory monocytes can differentiate into M2 macrophages via basophil-derived IL-4 (39). Moreover, it has been found that basophils produce a large amount of IL-4 in response to various stimulants, including IgE plus antigens, cytokines (IL-3, IL,18, and IL-33), and TLR ligands (40). Watanabe et al (17,18) demonstrated that TLR signaling in monocytes/macrophages and basophils might enhance the abnormal innate immune responses observed in IgG4-RD. A recent study showed infiltration of activated TLR-2+ and/or TLR-4+ basophils in the pancreas tissue of patients with autoimmune pancreatitis (41). Although the relationship between TLRs and innate immunity has recently received increasing attention with regard to the initiation of IgG4-RD, the detailed mechanism of pathogenesis by TLR signaling remains to be completely elucidated. Therefore, we performed gene expression microarray analysis to identify TLR-related molecules using SMG samples from patients with IgG4-RD and patients with chronic sialadenitis.

Microarray of SMGs demonstrated significant increases in TLR-7–, TLR-8–, and TLR-9–related genes in patients with IgG4-RD compared with patients with chronic sialadenitis and controls. In addition, overexpression of TLR-7 in SMGs from patients with IgG4-RD compared with the patients with chronic sialadenitis and controls was validated by real-time PCR and immunohistochemistry.

TLR-7 recognizes single-stranded RNA from viruses. Chang et al (37) observed IL-33 production by alveolar macrophages in virus-infected lungs after in vitro stimulation with an agonist of TLR-7, consistent with our results showing the positive correlation between TLR-7 and IL-33 only in IgG4-RD tissue. In addition, several studies have indicated that TLR-7 is important not only for the activation of antiviral responses but also for the induction of adaptive immunity (34). Activation of TLR-7–expressing plasmacytoid DCs in mice causes diseases such as lupus nephritis or arthritis (42), suggesting that TLR-7 has a risk of responding to endogenous ligands in the disease state. Notably, Yokogawa et al (43) showed that WT BALB/c mice treated with the TLR-7 agonist imiquimod for 4 weeks had an accumulation of plasmacytoid DCs at the epidermal–dermal junction and elevated serum IgG2a levels, but unchanged serum IgG1 levels. These results were consistent with our results in the present study (Figure 5I). Mouse IgG2a is the most prominent IgG subclass involved in inducing autoimmunity. Thus, Yokogawa et al suggested that mTLR-7 activation of plasmacytoid DCs in WT BALB/c mice leads to lupus-like systemic autoimmune disease.

On the other hand, Fukui et al (44), and the findings of the present study, showed a predominant infiltration of TLR-7+CD163+ M2 macrophages in the pancreas and SMGs from patients with IgG4-RD, while TLR-7+CD123+ plasmacytoid DCs were rarely seen in IgG4-RD tissues. Interestingly, the normal human secondary lymphoid organs, including lymph nodes and tonsils, showed a predominant infiltration of TLR-7+CD123+ plasmacytoid DCs. In huTLR-7–transgenic/mTLR-7$^{-/-}$ mice, fibrosis and lymphocytic
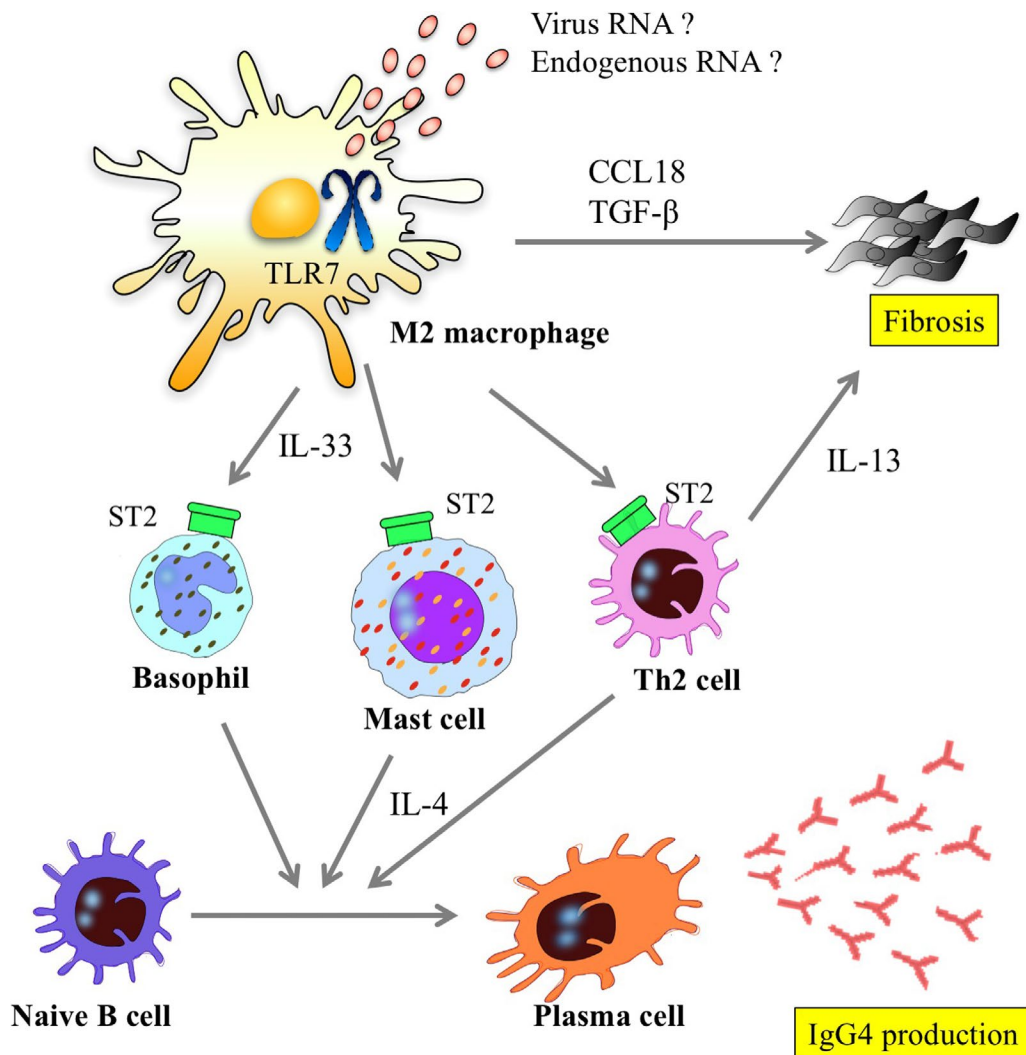
Figure 6. Schematic model of the role of Toll-like receptor 7 (TLR-7)–positive M2 macrophages in the initiation of Ig4-related disease. TLR-7 expressed on M2 macrophages recognize some RNA viruses or self RNA from apoptotic cells. Activated M2 macrophages secrete interleukin-33 (IL-33) and promote production of Th2 cytokines that lead to IgG4 class-switching and fibrosis. TGFβ = transforming growth factor β.

infiltration were notably increased in multiple organs compared with WT mice. Moreover, we confirmed elevated serum IgG and IgG1 levels in huTLR-7–transgenic/mTLR-7$^{-/-}$ mice after topical treatment with TLR-7 agonists. In contrast, Arai et al (45) reported that CD123+CD303+ plasmacytoid DCs were easily detected in pancreas tissues from patients with autoimmune pancreatitis. In addition, increased interferon-α production by plasmacytoid DCs promotes pancreatic inflammation in a murine model of autoimmune pancreatitis (MRL/Mp mice treated with the TLR-3 ligand poly[I–C]). These contradictions with the findings of previous studies are thought to reflect differences in TLR-7–expressing cells in each organ or in the function of mTLR-7 and huTLR-7.

This study is the first to demonstrate that huTLR-7 activation through topical TLR-7 agonist treatment in huTLR-7–transgenic/ mTLR-7$^{-/-}$ mice leads to an IgG4-RD phenotype. Furthermore, after topical treatment with TLR-7 agonists, fibrosis and lymphocytic infiltration in affected organs was notable. A schematic

model for the initiation of IgG4-RD is shown in Figure 6. M2 macrophages recognize some RNA viruses or self RNA from apoptotic cells in affected organs via TLR-7, which causes activated M2 macrophages to secrete IL-33 and promote production of Th2 cytokines by various immune cells that lead to IgG4 class-switching and severe fibrosis.

Since TLR-7 is considered to induce production of inflammatory cytokines (tumor necrosis factor, IL-1β, IL-12, and interferon-α) as well as IL-33, we are currently examining the association of novel T cell subsets, including CD4+ cytotoxic T cells and T follicular helper cells, with TLR-7 downstream signals other than IL-33 in both huTLR-7–transgenic/mTLR-7$^{-/-}$ mice and patients with IgG4-RD. A more thorough understanding of the role of TLR-7+CD163+ M2 macrophages in IgG4-RD could lead to the establishment of a mouse model of IgG4-RD and to the eventual development of novel pharmacologic strategies to interrupt TLR-7 or TLR-7 downstream

signals as a further means of inhibiting disease initiation or progression.

ACKNOWLEDGMENT

AUTHOR CONTRIBUTIONS

All authors were involved in drafting the article or revising it critically for important intellectual content, and all authors approved the final version to be published. Dr. Moriyama had full access to all of the data in the study and takes responsibility for the integrity of the data and the accuracy of the data analysis.
Study conception and design. Ishiguro, Moriyama.
Acquisition of data. Furusho, Furukawa, Chinju, Gion, Ohta, Maehara, Tanaka, Yamauchi, Sakamoto, Mochizuki, Ono.
Analysis and interpretation of data. Ishiguro, Moriyama, Shibata, Murakami, Haque, Hayashida, Sato, Kiyoshima, Yamamoto, Miyake, Nakamura.

REFERENCES

1. Hamano H, Kawa S, Horiuchi A, Unno H, Furuya N, Akamatsu T, et al. High serum IgG4 concentrations in patients with sclerosing pancreatitis. N Engl J Med 2001;344:732–8.

2. Umehara H, Okazaki K, Masaki Y, Kawano M, Yamamoto M, Saeki T, et al. A novel clinical entity, IgG4-related disease (IgG4RD): general concept and details. Mod Rheumatol 2012;22:1–14.

3. Stone JH, Zen Y, Deshpande V. IgG4-related disease. N Engl J Med 2012;366:539–51.

4. Nirula A, Glaser SM, Kalled SL, Taylor FR. What is IgG4? A review of the biology of a unique immunoglobulin subtype. Curr Opin Rheumatol 2011;23:119–24.

5. Finkelman FD, Boyce JA, Vercelli D, Rothenberg ME. Key advances in mechanisms of asthma, allergy, and immunology in 2009. J Allergy Clin Immunol 2010;125:312–8.

6. Meiler F, Klunker S, Zimmermann M, Akdis CA, Akdis M. Distinct regulation of IgE, IgG4 and IgA by T regulatory cells and Toll-like receptors. Allergy 2008;63:1455–63.

7. Maehara T, Moriyama M, Nakashima H, Miyake K, Hayashida JN, Tanaka A, et al. Interleukin-21 contributes to germinal centre formation and immunoglobulin G4 production in IgG4-related dacryoadenitis and sialoadenitis, so-called Mikulicz's disease. Ann Rheum Dis 2012;71:2011–9.

8. Tanaka A, Moriyama M, Nakashima H, Miyake K, Hayashida JN, Maehara T, et al. Th2 and regulatory immune reactions contribute to IgG4 production and the initiation of Mikulicz disease. Arthritis Rheum 2012;64:254–63.

9. Tsuboi H, Matsuo N, Iizuka M, Tsuzuki S, Kondo Y, Tanaka A, et al. Analysis of IgG4 class switch-related molecules in IgG4-related disease. Arthritis Res Ther 2012;14:R171.

10. Zen Y, Fujii T, Harada K, Kawano M, Yamada K, Takahira M, et al. Th2 and regulatory immune reactions are increased in immunoglobin G4-related sclerosing pancreatitis and cholangitis. Hepatology 2007;45:1538–46.

11. Moriyama M, Tanaka A, Maehara T, Furukawa S, Nakashima H, Nakamura S. T helper subsets in Sjögren's syndrome and IgG4-related dacryoadenitis and sialoadenitis: a critical review. J Autoimmun 2014;51:81–8.

12. Akiyama M, Suzuki K, Yamaoka K, Yasuoka H, Takeshita M, Kaneko Y, et al. Number of circulating follicular helper 2 T cells correlates with IgG4 and interleukin-4 levels and plasmablast numbers in IgG4-related disease. Arthritis Rheumatol 2015;67:2476–81.

13. Maehara T, Mattoo H, Ohta M, Mahajan VS, Moriyama M, Yamauchi M, et al. Lesional CD4+ IFN-γ+ cytotoxic T lymphocytes in IgG4-related dacryoadenitis and sialoadenitis. Ann Rheum Dis 2017;76:377–85.

14. Mattoo H, Mahajan VS, Della-Torre E, Sekigami Y, Carruthers M, Wallace ZS, et al. De novo oligoclonal expansions of circulating plasmablasts in active and relapsing IgG4-related disease. J Allergy Clin Immunol 2014;134:679–87.

15. Furukawa S, Moriyama M, Tanaka A, Maehara T, Tsuboi H, Iizuka M, et al. Preferential M2 macrophages contribute to fibrosis in IgG4-related dacryoadenitis and sialoadenitis, so-called Mikulicz's disease. Clin Immunol 2015;156:9–18.

16. Furukawa S, Moriyama M, Miyake K, Nakashima H, Tanaka A, Maehara T, et al. Interleukin-33 produced by M2 macrophages and other immune cells contributes to Th2 immune reaction of IgG4-related disease. Sci Rep 2017;7:42413.

17. Watanabe T, Yamashita K, Fujikawa S, Sakurai T, Kudo M, Shiokawa M, et al. Involvement of activation of Toll-like receptors and nucleotide-binding oligomerization domain-like receptors in enhanced IgG4 responses in autoimmune pancreatitis. Arthritis Rheum 2012;64:914–24.

18. Watanabe T, Yamashita K, Sakurai T, Kudo M, Shiokawa M, Uza N, et al. Toll-like receptor activation in basophils contributes to the development of IgG4-related disease. J Gastroenterol 2013;48:247–53.

19. Mackay F, Browning JL. BAFF: a fundamental survival factor for B cells. Nat Rev Immunol 2002;2:465–75.

20. Janeway CA Jr, Medzhitov R. Innate immune recognition. Annu Rev Immunol 2002;20:197–216.

21. Beutler B, Rietschel ET. Innate immune sensing and its roots: the story of endotoxin. Nat Rev Immunol 2003;3:169–76.

22. Medzhitov R. Toll-like receptors and innate immunity. Nat Rev Immunol 2001;1:135–45.

23. Akira S, Takeda K, Kaisho T. Toll-like receptors: critical proteins linking innate and acquired immunity. Nat Immunol 2001;2:675–80.

24. Hwang IY, Park C, Harrison K, Kehrl JH. TLR4 signaling augments B lymphocyte migration and overcomes the restriction that limits access to germinal center dark zones. J Exp Med 2009;206:2641–57.

25. Moriyama M, Furukawa S, Kawano S, Goto Y, Kiyoshima T, Tanaka A, et al. The diagnostic utility of biopsies from the submandibular and labial salivary glands in IgG4-related dacryoadenitis and sialoadenitis, so-called Mikulicz's disease. Int J Oral Maxillofac Surg 2014;43:1276–81.

26. Umehara H, Okazaki K, Masaki Y, Kawano M, Yamamoto M, Saeki T, et al. Comprehensive diagnostic criteria for IgG4-related disease (IgG4-RD), 2011. Mod Rheumatol 2012;22:21–30.

27. Masaki Y, Sugai S, Umehara H. IgG4-related diseases including Mikulicz's disease and sclerosing pancreatitis: diagnostic insights. J Rheumatol 2010;37:1380–5.

28. Fujibayashi T, Sugai S, Miyasaka N, Hayashi Y, Tsubota K. Revised Japanese criteria for Sjögren's syndrome (1999): availability and validity. Mod Rheumatol 2004;14:425–34.

29. Shiboski CH, Shiboski SC, Seror R, Criswell LA, Labetoulle M, Lietman TM, et al, and the International Sjögren's Syndrome Criteria Working Group. 2016 American College of Rheumatology/European League Against Rheumatism classification criteria for primary Sjögren's syndrome: a consensus and data-driven methodology involving three international patient cohorts. Arthritis Rheumatol 2017;69:35–45.

30. Moriyama M, Hayashida JN, Toyoshima T, Ohyama Y, Shinozaki S, Tanaka A, et al. Cytokine/chemokine profiles contribute to

understanding the pathogenesis and diagnosis of primary Sjögren's syndrome. Clin Exp Immunol 2012;169:17–26.

31. Ohta M, Moriyama M, Maehara T, Gion Y, Furukawa S, Tanaka A, et al. DNA microarray analysis of submandibular glands in IgG4-related disease indicates a role for MARCO and other innate immune-related proteins. Medicine (Baltimore) 2016;95:e2853.

32. Greenspan JS, Daniels TE, Talal N, Sylvester RA. The histopathology of Sjögren's syndrome in labial salivary gland biopsies. Oral Surg Oral Med Oral Pathol 1974;37:217–29.

33. Chisholm DM, Mason DK. Labial salivary gland biopsy in Sjögren's disease. J Clin Pathol 1968;21:656–60.

34. Baenziger S, Heikenwalder M, Johansen P, Schlaepfer E, Hofer U, Miller RC, et al. Triggering TLR7 in mice induces immune activation and lymphoid system disruption, resembling HIV-mediated pathology. Blood 2009;113:377–88.

35. Schmitz J, Owyang A, Oldham E, Song Y, Murphy E, McClanahan TK, et al. IL-33, an interleukin-1-like cytokine that signals via the IL-1 receptor-related protein ST2 and induces T helper type 2-associated cytokines. Immunity 2005;23:479–90.

36. Louten J, Rankin AL, Li Y, Murphy EE, Beaumont M, Moon C, et al. Endogenous IL-33 enhances Th2 cytokine production and T-cell responses during allergic airway inflammation. Int Immunol 2011;23:307–15.

37. Chang YJ, Kim HY, Albacker LA, Baumgarth N, McKenzie AN, Smith DE, et al. Innate lymphoid cells mediate influenza-induced airway hyper-reactivity independently of adaptive immunity. Nat Immunol 2011;12:631–8.

38. Paul WE, Zhu J. How are T_H2-type immune responses initiated and amplified? Nat Rev Immunol 2010;10:225–35.

39. Egawa M, Mukai K, Yoshikawa S, Iki M, Mukaida N, Kawano Y, et al. Inflammatory monocytes recruited to allergic skin acquire an anti-inflammatory M2 phenotype via basophil-derived interleukin-4. Immunity 2013;38:570–80.

40. Yamanishi Y, Karasuyama H. Basophil-derived IL-4 plays versatile roles in immunity. Semin Immunopathol 2016;38:615–22.

41. Yanagawa M, Uchida K, Ando Y, Tomiyama T, Yamaguchi T, Ikeura T, et al. Basophils activated via TLR signaling may contribute to pathophysiology of type 1 autoimmune pancreatitis. J Gastroenterol 2018;53:449–60.

42. Deane JA, Pisitkun P, Barrett RS, Feigenbaum L, Town T, Ward JM, et al. Control of Toll-like receptor 7 expression is essential to restrict autoimmunity and dendritic cell proliferation. Immunity 2007;27:801–10.

43. Yokogawa M, Takaishi M, Nakajima K, Kamijima R, Fujimoto C, Kataoka S, et al. Epicutaneous application of Toll-like receptor 7 agonists leads to systemic autoimmunity in wild-type mice: a new model of systemic lupus erythematosus. Arthritis Rheumatol 2014;66:694–706.

44. Fukui Y, Uchida K, Sakaguchi Y, Fukui T, Nishio A, Shikata N, et al. Possible involvement of Toll-like receptor 7 in the development of type 1 autoimmune pancreatitis. J Gastroenterol 2015;50:435–44.

45. Arai Y, Yamashita K, Kuriyama K, Shiokawa M, Kodama Y, Sakurai T, et al. Plasmacytoid dendritic cell activation and IFN-α production are prominent features of murine autoimmune pancreatitis and human IgG4-related autoimmune pancreatitis. J Immunol 2015;195:3033–44.